

# Dash: Semi-Supervised Learning with Dynamic Thresholding

Yi Xu <sup>\*1</sup>, Lei Shang <sup>†1</sup>, Jinxing Ye <sup>‡1</sup>, Qi Qian <sup>§1</sup>, Yu-Feng Li <sup>¶2</sup>, Baigui Sun <sup>||1</sup>, Hao Li <sup>\*\*1</sup>,  
and Rong Jin <sup>††1</sup>

<sup>1</sup>Machine Intelligence Technology, Alibaba Group

<sup>2</sup>National Key Laboratory for Novel Software Technology, Nanjing University

September 3, 2021

## Abstract

While semi-supervised learning (SSL) has received tremendous attentions in many machine learning tasks due to its successful use of unlabeled data, existing SSL algorithms use either all unlabeled examples or the unlabeled examples with a fixed high-confidence prediction during the training progress. However, it is possible that too many correct/wrong pseudo labeled examples are eliminated/selected. In this work we develop a simple yet powerful framework, whose key idea is to select a subset of training examples from the unlabeled data when performing existing SSL methods so that only the unlabeled examples with pseudo labels related to the labeled data will be used to train models. The selection is performed at each updating iteration by only keeping the examples whose losses are smaller than a given threshold that is dynamically adjusted through the iteration. Our proposed approach, Dash, enjoys its adaptivity in terms of unlabeled data selection and its theoretical guarantee. Specifically, we theoretically establish the convergence rate of Dash from the view of non-convex optimization. Finally, we empirically demonstrate the effectiveness of the proposed method in comparison with state-of-the-art over benchmarks.

## 1 Introduction

In spite of successful use in a variety of classification and regression tasks, supervised learning requires large amount of *labeled* training data. In many machine learning applications, labeled data can be significantly more costly, time-consuming and difficult to obtain than the *unlabeled* data [Zhu, 2005], since they usually require experienced human labors from experts (e.g., a doctor in detection of covid-19 by using X-ray images). Typically, only a small amount of labeled data is available, but there is a huge amount of data without label. This is one of key hurdles in the development and deployment of machine learning models.

Semi-supervised learning (SSL) is designed to improve learning performance by leveraging an abundance of unlabeled data along with limited labeled data [Chapelle et al., 2006]. In much recent work, SSL can be categorized into several main classes in terms of the use of unlabeled data: consistency regularization, pseudo labeling, generic regularization (e.g., large margin regularization, Laplacian regularization, etc [Chapelle

---

\*yixu@alibaba-inc.com

†sl172005@alibaba-inc.com

‡zhengze.yjx@alibaba-inc.com

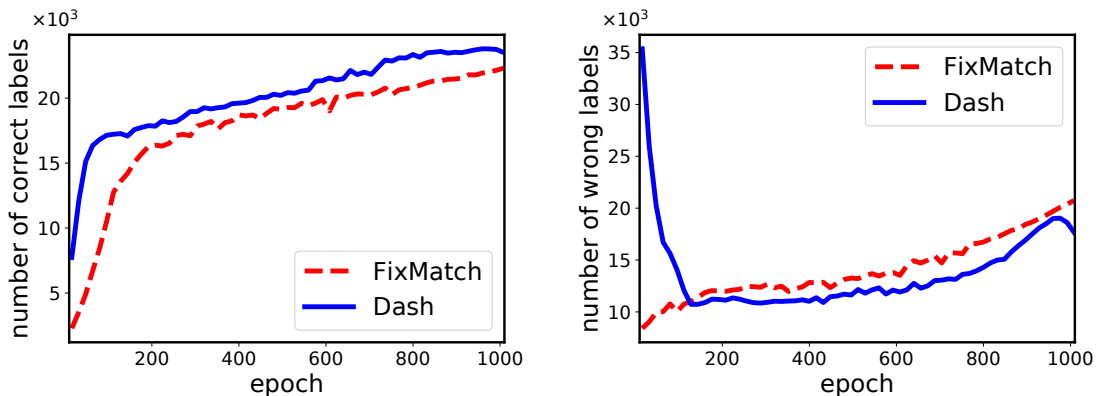
§qi.qian@alibaba-inc.com

¶liyf@nju.edu.cn

||baigui.sbg@alibaba-inc.com

\*\*lihao.lh@alibaba-inc.com

††jinrong.jr@alibaba-inc.com



(a) Number of selected unlabeled examples with correct pseudo labels (b) Number of selected unlabeled examples with wrong pseudo labels

Figure 1: An example of experimental results on Wide ResNet-28-8 for CIFAR-100 with 400 labeled images illustrates the reason of dynamically selecting unlabeled data to train learning models. Pseudo labels are generated based on the prediction models. FixMatch selects unlabeled example if its confidence prediction is greater than 0.95, while the proposed Dash algorithm selects unlabeled example based on a dynamic threshold through optimization iterations. (a) The proposed Dash selects more examples with correct pseudo labels than that of FixMatch. (b) The proposed Dash maintains much more examples with wrong pseudo labels at the beginning but it will drop off more examples with wrong pseudo labels after several epochs, comparing to FixMatch.

et al., 2006]), and their combinations. With the image data augmentation technique, consistency regularization uses unlabeled data [Baird, 1992, Schmidhuber, 2015] based on the condition that the model predictions between different perturbed versions of the same image are similar. Another line of work is to produce artificial label for unlabeled data based on prediction model and add them to the training data set. With different approaches of artificial label production, varies of SSL methods have been proposed in the literature including self-training [Yarowsky, 1995, Lee, 2013, Rosenberg et al., 2005, Sajjadi et al., 2016, Laine and Aila, 2017, Xie et al., 2020b] and co-training [Blum and Mitchell, 1998, Zhou and Li, 2005, Sindhwani and Rosenberg, 2008, Wang et al., 2008, Yu et al., 2008, Wang and Zhou, 2010, Chen et al., 2011]. Due to its capability to handle both labeled data and unlabeled data, SSL has been widely studied in diverse machine learning tasks such as image classification [Sajjadi et al., 2016, Laine and Aila, 2017, Tarvainen and Valpola, 2017, Xie et al., 2020a, Berthelot et al., 2019b,a], natural language processing [Turian et al., 2010], speech recognition [Yu et al., 2010], and object detection [Misra et al., 2015].

Numerous empirical evidences show that unlabeled data in SSL can help to improve the learning performance [Berthelot et al., 2019b,a, Sohn et al., 2020], however, a series of theoretical studies [Ben-David et al., 2008, Singh et al., 2009, Li and Zhou, 2011b, Balcan and Blum, 2005] have demonstrated that this success is highly relying on a necessary condition that labeled data and unlabeled data with pseudo label come from the same distribution during the training process [Zhu, 2005, Van Engelen and Hoos, 2020]. Unfortunately, it has been shown that this condition does not always hold in real applications and thus it could hurt the performance [Li et al., 2017, Oliver et al., 2018]. For example, the pseudo label of an unlabeled example generated by conventional SSL methods during the training progress is not correct [Hataya and Nakayama, 2019, Li et al., 2020]. In this case, the degradation of model performance has been observed when using unlabeled data compared to the simple supervised learning model not using any unlabeled data at all [Chapelle et al., 2006, Oliver et al., 2018]. Thus, not all unlabeled data are needed in SSL.

To improve SSL performance, multiple studies [Guo et al., 2020, Ren et al., 2020] examined the strategies of weighting different training unlabeled examples by solving a bi-level optimization problem. It is also

a popular idea to select a subset of training examples from unlabeled examples for SSL. For example, FixMatch [Sohn et al., 2020] uses the unlabeled examples with a fixed high-confidence prediction (e.g., 0.95) in classification tasks using cross entropy loss. However, the fixed threshold may lead to eliminate too many unlabeled examples with correct pseudo labels (see Figure 1 (a)) and may lead to select too many unlabeled examples with wrong pseudo labels (see Figure 1 (b)). That is to say, the fixed threshold is possible not good enough during the training progress and thus it could degrade the overall performance.

Unlike the previous work, we aim to the proposed approach enjoys its adaptivity in terms of unlabeled data selection and its theoretical guarantee. This inspires us to consider answering the following question in this study.

**Can we design a provable SSL algorithm that selects unlabeled data with dynamic thresholding?**

To this end, we propose a generic SSL algorithm with **Dynamic Thresholding** (Dash) that can dynamically select unlabeled data during the training process. Specifically, Dash firstly runs over labeled data and obtains a threshold for unlabeled data selection. It then selects the unlabeled data whose loss values are smaller than the threshold to the training data-set. The value of threshold is gradually decreased over the optimization iterations. It can be integrated with existing SSL methods like FixMatch [Sohn et al., 2020]. From the view of optimization, we show that eventually the proposed Dash can non-asymptotically converge with theoretical guarantee. Empirical evaluations on image benchmarks validate the effectiveness of Dash comparing with the state-of-the-art SSL algorithms.

## 2 Related Work

There has been growing interest in semi-supervised learning for training machine learning and deep learning [Flach, 2012, Goodfellow et al., 2016]. A number of SSL methods have been studied by leveraging the structure of unlabeled data including consistency regularization [Bachman et al., 2014, Sajjadi et al., 2016, Laine and Aila, 2017, Tarvainen and Valpola, 2017, Miyato et al., 2018, Xie et al., 2020a], entropy minimization [Grandvalet and Bengio, 2005, Lee, 2013], and other interesting approaches [Berthelot et al., 2019b,a]. In addition, several studies on SSL have been proposed to keep SSL performing safe when using unlabeled data, which is known as safe SSL [Li and Zhou, 2015]. An non-exhaustive list of those studies include [Cozman et al., 2003, Singh et al., 2009, Li and Zhou, 2011a, Balsubramani and Freund, 2015, Loog, 2015, Li et al., 2017, Krijthe and Loog, 2017, Li et al., 2021, Mey and Loog, 2019, Guo et al., 2020]. For example, Ren et al. [2020] proposed a new SSL framework that uses an individual weight for each unlabeled example, and it updates the individual weights and models iteratively by solving a bi-level optimization problem approximately. In this paper, we mainly focus on improved deep SSL methods with the use of unlabeled data selection. Comprehensive surveys on SSL methods could be refer to [Zhu, 2005, Chapelle et al., 2006, Zhu and Goldberg, 2009, Hady and Schwenker, 2013, Van Engelen and Hoos, 2020].

The use of unlabeled data selection by a threshold is not new in the literature of SSL. As a simple yet widely used heuristic algorithm, pseudo-labeling [Lee, 2013] (a.k.a. self-training [McLachlan, 1975, Yarowsky, 1995, Rosenberg et al., 2005, Sajjadi et al., 2016, Laine and Aila, 2017, Xie et al., 2020b]) uses the prediction model itself to generate pseudo labels for unlabeled images. Then the unlabeled images whose corresponding pseudo label’s highest class probability is larger than a predefined threshold will be used for the training. Nowadays, pseudo-labeling has been become an important component of many modern SSL methods [Xie et al., 2020a, Sohn et al., 2020].

With the use of weak and strong data augmentations, several recent works such as UDA [Xie et al., 2020a], ReMixMatch [Berthelot et al., 2019a] and FixMatch [Sohn et al., 2020] have been proposed in image classification problems. Generally, they use a weakly-augmented <sup>1</sup> unlabeled image to generate a pseudo label and enforce consistency against strongly-augmented <sup>2</sup> version of the same image. In particular,

<sup>1</sup>Both UDA and ReMixMatch use crop and flip as “weak” augmentation while FixMatch uses flip and shift.

<sup>2</sup>For “strong” augmentation, UDA uses RandAugment [Cubuk et al., 2020], ReMixMatch uses CTAugment [Cubuk et al., 2019], and FixMatch uses both.

UDA and FixMatch use a fixed threshold to retain the unlabeled example whose highest probability in the predicted class distribution for the pseudo label is higher than the threshold. For example, UDA sets this threshold to be 0.8 for CIFAR-10 and SVHN, and FixMatch sets the threshold to be 0.95 for all data-sets. To encourage the model to generate high-confidence predictions, UDA and ReMixMatch sharpen the guessed label distribution by adjusting its temperature and then re-normalize the distribution. [Sohn et al. \[2020\]](#) have shown that the sharpening and thresholding pseudo-labeling have a similar effect.

By contrast, the proposed Dash method selects a subset of unlabeled data to be used in training models by a data-dependent dynamic threshold, and its theoretical convergence guarantee is established for stochastic gradient descent under the non-convex setting, which is applicable to deep learning.

## 3 Preliminary and Background

### 3.1 Problem Setting

We study the task of learning a model to map an input  $\mathbf{x} \in \mathcal{X} \subseteq \mathbb{R}^d$  onto a label  $\mathbf{y} \in \mathcal{Y}$ . In many machine learning applications,  $\mathbf{x}$  refers to the feature and  $\mathbf{y} \in \mathcal{Y}$  refers to the label for classification or regression. For simplicity, let  $\xi$  denote the input-label pair  $(\mathbf{x}, \mathbf{y})$ , i.e.  $\xi := (\mathbf{x}, \mathbf{y})$ . We denote by  $\mathcal{P}$  the underlying distribution of data pair  $\xi$ , then  $\xi \sim \mathcal{P}$ . The goal is to learn a model  $\mathbf{w} \in \mathbb{R}^d$  via minimizing an optimization problem whose objective function  $F(\mathbf{w})$  is the expectation of random loss function  $f(\mathbf{w}; \xi)$ :

$$\min_{\mathbf{w} \in \mathbb{R}^d} F(\mathbf{w}) := \mathbb{E}_{\xi \sim \mathcal{P}} [f(\mathbf{w}; \xi)], \quad (1)$$

where  $\mathbb{E}_{\xi}[\cdot]$  is an expectation taking over random variable  $\xi \sim \mathcal{P}$ . The optimization problem (1) covers most machine learning and deep learning applications. In this paper, we consider the classification problem with  $K$ -classes, whose loss function is the cross-entropy loss given by

$$f(\mathbf{w}; \xi_i) = H(\mathbf{y}_i, \mathbf{p}(\mathbf{w}; \mathbf{x}_i)) := \sum_{k=1}^K -y_{i,k} \log \left( \frac{\exp(p_k(\mathbf{w}; \mathbf{x}_i))}{\sum_{j=1}^K \exp(p_j(\mathbf{w}; \mathbf{x}_i))} \right), \quad (2)$$

where  $\mathbf{p}(\mathbf{w}; \mathbf{x})$  is the prediction function and  $H(\mathbf{q}, \mathbf{p})$  is the cross-entropy between  $\mathbf{q}$  and  $\mathbf{p}$ . In this paper, we do not require the function  $f(\mathbf{w}; \xi)$  to be convex in terms of  $\mathbf{w}$ , which is applicable to various deep learning tasks.

In SSL, it consists of labeled examples and unlabeled examples. Let

$$\mathbf{D}_l := \{(\mathbf{x}_i, \mathbf{y}_i), i = 1, \dots, N_l\} \quad (3)$$

be the labeled training data. Given unlabeled training examples  $\{\mathbf{x}_i^u, i = 1, 2, \dots, N_u\}$ , one can generate pseudo label  $\hat{\mathbf{y}}_i^u$  based on the predictions of a supervised model on labeled data. Different SSL methods such as pseudo-labeling [[Lee, 2013](#)], Adversarial Training [[Miyato et al., 2018](#)], UDA [[Xie et al., 2020a](#)], and FixMatch [[Sohn et al., 2020](#)] have been proposed to generate pseudo labels. We denote by

$$\mathbf{D}_u := \{(\mathbf{x}_i^u, \hat{\mathbf{y}}_i^u), i = 1, \dots, N_u\} \quad (4)$$

the unlabeled data, where  $\hat{\mathbf{y}}_i^u \in \mathcal{Y}$  is the pseudo label. Although it contains pseudo label, we still call  $\mathbf{D}_u$  unlabeled data for simplicity in our analysis. Usually, the number of unlabeled examples is much larger than the number of labeled examples, i.e.,  $N_u \gg N_l$ . Finally, the training data consists of labeled data  $\mathbf{D}_l$  and unlabeled data with pseudo label  $\mathbf{D}_u$ , and thus the training loss of an SSL algorithm usually contains supervised loss  $F_s$  and unsupervised loss  $F_u$  with a weight  $\lambda_u > 0$ :  $F_s + \lambda_u F_u$ , where  $F_s$  is constructed on  $\mathbf{D}_l$  and  $F_u$  is constructed on  $\mathbf{D}_u$ . In image classification problems,  $F_s$  is just the standard cross-entropy loss:

$$F_s(\mathbf{w}) := \frac{1}{N_l} \sum_{i=1}^{N_l} f(\mathbf{w}; \xi_i), \quad (5)$$

where  $\xi_i \in \mathbf{D}_l$  and  $f$  is defined in (2). Thus, different constructions of the unsupervised loss  $F_u$  lead to different SSL methods. Typically, there are two ways of constructing  $F_u$ : one is to use pseudo labels to formulate a “supervised” loss such as cross-entropy loss (e.g., FixMatch), and another one is to optimize a regularization that does not depend on labels such as consistency regularization (e.g.,  $\Pi$ -Model). Next, we will introduce a recent SSL work to interpret how to generate pseudo labels and construct unsupervised loss  $F_u$ .

### 3.2 FixMatch: An SSL Algorithm with Fixed Thresholding

Due to its simplicity yet empirical success, we select FixMatch [Sohn et al., 2020] as an SSL example in this subsection. Besides, we consider FixMatch as a warm-up of the proposed algorithm, since FixMatch uses a fixed threshold to retain unlabeled examples and it will be used as a pipeline in the proposed algorithm.

The key idea of FixMatch is to use a separate weak and strong augmentation when generating model’s predicted class distribution and one-hot label in unsupervised loss. Specifically, based on a supervised model  $\mathbf{w}$  and a weak augmentation  $\alpha$ , FixMatch predict the class distribution

$$\mathbf{h}_i = \mathbf{p}(\mathbf{w}, \alpha(\mathbf{x}_i^u)) \quad (6)$$

for a weakly-augmented version of a unlabeled image  $\mathbf{x}_i^u$ , where  $\mathbf{p}(\mathbf{w}, \mathbf{x})$  is the prediction function. Then it creates a pseudo label by

$$\hat{\mathbf{y}}_i^u = \arg \max(\mathbf{h}_i). \quad (7)$$

Following by [Sohn et al., 2020], the arg max applied to a probability distribution produces a “one-hot” probability distribution. To construct the unsupervised loss, it computes the model prediction for a strong augmentation  $\mathcal{T}$  of the same unlabeled image  $\mathbf{x}_i^u$ :

$$\mathbf{p}(\mathbf{w}, \mathcal{T}(\mathbf{x}_i^u)). \quad (8)$$

The unsupervised loss is defined as the cross-entropy between  $\hat{\mathbf{y}}_i^u$  and  $\mathbf{p}_i$ :

$$H(\hat{\mathbf{y}}_i^u, \mathbf{p}(\mathbf{w}, \mathcal{T}(\mathbf{x}_i^u))). \quad (9)$$

Eventually, FixMatch only uses the unlabeled examples with a high-confidence prediction by selecting based on a **fixed threshold**  $\tau = 0.95$ . Therefore, in FixMatch the cross-entropy loss with pseudo-label and confidence for unlabeled data is given by

$$F_u(\mathbf{w}) = \frac{1}{N_u} \sum_{i=1}^{N_u} I(\max(\mathbf{h}_i) \geq \tau) H(\hat{\mathbf{y}}_i^u, \mathbf{p}(\mathbf{w}, \mathcal{T}(\mathbf{x}_i^u))), \quad (10)$$

where  $I(\cdot)$  is an indicator function.

As we discussed in introduction, this fixed threshold may lead to eliminate/select too many unlabeled examples with correct/wrong pseudo labels (see Figure 1), which eventually could drop off overall performance. It is a natural choice: the threshold is not fixed across the optimization iterations. Thus, in the next section, we are going to propose a new SSL scheme having a dynamic threshold.

## 4 Dash: An SSL Algorithm with Dynamic Thresholding

Before introducing the proposed method, we would like to point out the importance of unlabeled data selection in SSL from the theoretical view of optimization. Classical SSL methods [Zhu, 2005, Chapelle et al., 2006, Zhu and Goldberg, 2009, Hady and Schwenker, 2013, Van Engelen and Hoos, 2020] assume that labeled data and unlabeled data are from the same distribution. That is to say,  $\xi \sim \mathcal{P}$  holds for  $\xi \in \mathbf{D}_l \cup \mathbf{D}_u$ . Then SSL methods aim to solve the optimization problem (1) by using a standard stochastic optimization

---

**Algorithm 1** Dash: Semi-Supervised Learning with **D**ynamic **T**hresholding

---

Input: learning rate  $\eta_0$  and mini-batch size  $m_0$  for stage one, learning rate  $\eta$  and parameter  $m$  of mini-batch size for stage two, two parameters  $C > 1$  and  $\gamma > 1$  for computing threshold, and violation probability  $\delta$ .

// Warm-up Stage: run SGD in  $T_0$  iterations.

Initialization:  $\mathbf{u}_0 = \mathbf{w}_0$

**for**  $t = 0, 1, \dots, T_0 - 1$  **do**

    Sample  $m_0$  examples  $\xi_{t,i}$  ( $i = 1, \dots, m_0$ ) from  $\mathbf{D}_l$ ,

$\mathbf{u}_{t+1} = \mathbf{u}_t - \eta_0 \tilde{\mathbf{g}}_t$  where  $\tilde{\mathbf{g}}_t = \frac{1}{m_0} \sum_{i=1}^{m_0} \nabla f_s(\mathbf{u}_t; \xi_{t,i})$

**end for**

// Selection Stage: run SGD in  $T$  iterations.

Initialization:  $\mathbf{w}_1 = \mathbf{u}_{T_0}$ .

Compute the value of  $\hat{\rho}$  as in (16). // In practice,  $\hat{\rho}$  can be obtained as in (17).

**for**  $t = 1, \dots, T$  **do**

    1) Sample  $n_t = m\gamma^{t-1}$  examples from  $\mathbf{D}_u$ , where the pseudo labels in  $\mathbf{D}_u$  are generated by FixMatch

    2) Set the threshold  $\rho_t = C\gamma^{-(t-1)}\hat{\rho}$ .

    3) Compute truncated stochastic gradient  $\mathbf{g}_t$  as (18).

    4) Update solution by SGD using stochastic gradient  $\mathbf{g}_t$  and learning rate  $\eta$ :  $\mathbf{w}_{t+1} = \mathbf{w}_t - \eta\mathbf{g}_t$ .

**end for**

Output:  $\mathbf{w}_{T+1}$

---

algorithm like mini-batch stochastic gradient descent (SGD). Specifically, at iteration  $t$ , mini-batch SGD updates intermediate solutions by

$$\mathbf{w}_{t+1} = \mathbf{w}_t - \frac{\eta}{m} \sum_{i=1}^m \nabla f(\mathbf{w}_t; \xi_{t,i}), \quad (11)$$

where  $m$  is the mini-batch size,  $\xi_{t,i}$  is sampled from training data  $\mathbf{D}_l \cup \mathbf{D}_u$ ,  $\nabla f(\mathbf{w}; \xi)$  is the gradient of  $f(\mathbf{w}; \xi)$  in terms of  $\mathbf{w}$ . In this situation, the theoretical convergence guarantee of SSL algorithms can be simply established under mild assumptions on objective function  $f(\mathbf{w}; \xi)$  such as smoothness and bounded variance [Ghadimi et al., 2016]. If the labeled data and unlabeled data are not from the same distribution such as some of pseudo labels are not correct, classical SSL methods with standard stochastic optimization algorithm may lead to the performance drops [Chapelle et al., 2006, Oliver et al., 2018]. Besides, the theoretical guarantee of the optimization algorithm for this case is not clear. This inspires us to design a new algorithm to overcome this issue. To this end, we proposed an SSL method that can dynamically select unlabeled examples during the training progress.

First, let us define the loss function for the proposed method. Same as FixMatch, the supervised loss  $F_s(\mathbf{w})$  for the proposed method is the standard cross-entropy loss on labeled data  $\mathbf{D}_l$ :

$$F_s(\mathbf{w}) := \frac{1}{N_l} \sum_{i=1}^{N_l} f_s(\mathbf{w}; \xi_i), \quad (12)$$

where  $\xi_i = (\mathbf{x}_i, \mathbf{y}_i)$  is sampled from  $\mathbf{D}_l$ ,  $f_s(\mathbf{w}; \xi_i) = H(\mathbf{y}_i, \mathbf{p}(\mathbf{w}; \alpha(\mathbf{x}_i)))$ , and  $\alpha(\mathbf{x})$  is the weakly-augmented version of  $x$ . Since the new dynamic threshold is not fixed, we let it rely on the optimization iteration  $t$  and it is denoted by  $\rho_t$ . Then the unsupervised loss is given by

$$F_u(\mathbf{w}) = \frac{1}{N_u} \sum_{i=1}^{N_u} I(f_u(\mathbf{w}; \xi_i^u) \leq \rho_t) f_u(\mathbf{w}; \xi_i^u), \quad (13)$$

where  $\xi_i^u = (\mathbf{x}_i^u, \hat{\mathbf{y}}_i^u)$  is sampled from  $\mathbf{D}_u$ ,  $f_u(\mathbf{w}; \xi_i^u) = H(\hat{\mathbf{y}}_i^u, \mathbf{p}(\mathbf{w}; \mathcal{T}(\mathbf{x}_i^u)))$ ,  $\mathcal{T}(x)$  is the strongly-augmented version of  $x$ , and the pseudo label  $\hat{\mathbf{y}}_i^u$  is generated based on (6) and (7) using prediction model  $\mathbf{w}$  and a

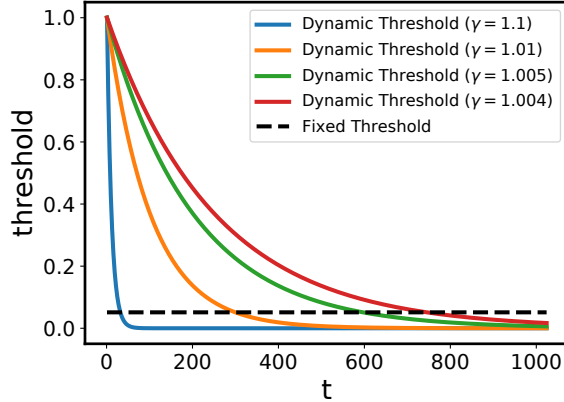


Figure 2: Comparison of fixed threshold and dynamic threshold. Fixed threshold is in the scale of negative log:  $-\log(0.95)$ , dynamic threshold  $\rho_t = 1.0001\gamma^{-(t-1)}$ .

unlabeled image  $\mathbf{x}_i^u$ . The unsupervised loss (13) shows that the Dash will retain the unlabeled example whose loss is smaller than the threshold  $\rho_t$ . If we rewrite the indicator function  $I(\max(\mathbf{h}_i) \geq \tau)$  in (10) to an equivalent expression

$$I(-\log(\max(\mathbf{h}_i)) \leq -\log(\tau)), \quad (14)$$

we can consider  $-\log(\max(\mathbf{h}_i))$  as a cross-entropy loss for one-hot label. Roughly speaking, FixMatch retains the unlabeled images with the loss  $-\log(\max(\mathbf{h}_i))$  smaller than  $-\log(0.95) \approx 0.0513$ . It is worth nothing that the loss  $-\log(\max(\mathbf{h}_i))$  contains the information of weakly-augmented images, while the loss  $f_u(\mathbf{w}; \xi_i^u)$  in (13) includes the information of both weakly-augmented and strongly-augmented images, meaning that the proposed method considers the entire loss function.

We then need to construct  $\rho_t$ . Intuitively, with the increase of the optimization iteration  $t$ , the loss function would decrease in general, so that  $\rho_t$  is also required to decrease. Mathematically, we set the **dynamic threshold**  $\rho_t$  as a decreasing function of  $t$ , which is given by

$$\rho_t := C\gamma^{-(t-1)}\hat{\rho}, \quad (15)$$

where  $C > 1, \gamma > 1$  are two constants. For example, we set  $C = 1.0001$  in our experiments and thus at first iteration (i.e.,  $t = 1$ ) the unlabeled examples whose loss values are smaller than  $\rho_t = 1.0001 \times \hat{\rho}$  will be used in the training. Figure 2 shows a comparison of fixed threshold used in FixMatch and dynamic threshold  $\rho_t$  in (15) with  $C = 1.0001, \hat{\rho} = 1$  and different  $\gamma$ , where the threshold in FixMatch is in the scale of negative log. It seems our thresholding strategy matches the curve of training loss in many real applications (e.g., see Figure 1 (a) of [Zhang et al., 2017]).

Next, it is important to estimate the value of  $\hat{\rho}$ . In theory, it can be estimated by

$$\hat{\rho} = \max \left\{ a, \frac{4G^2(1 + \delta b_0 m)}{\delta \mu a_0 m} \right\}, \quad (16)$$

where contains several parameters related to the property of considered problem (1) whose detailed definitions can be found in Theorem 1. Please note that the estimation of  $\hat{\rho}$  in (16) is for the use of convergence analysis only. In practice, we can use the following averaged loss from the training set  $\mathbf{D}_l$  as the approximate  $\hat{\rho}$ :

$$\hat{\rho} \approx \frac{1}{|\mathbf{D}_l|} \sum_{\xi_i \in \mathbf{D}_l} f(\mathbf{w}_1; \xi_i), \quad (17)$$

where  $|\mathbf{D}_l|$  is the number of examples in  $\mathbf{D}_l$ , and  $\mathbf{w}_1$  can be learned on  $\mathbf{D}_l$ . We can see from (17) with (13) and (15) that the unlabeled examples whose losses are smaller than the averaged loss of labeled examples will be maintained during the training process.

Finally, it is ready to describe the proposed Dash algorithm in details that contains two stages: warm-up stage and selection stage. In the warm-up stage, it runs SGD to train a model over labeled data  $\mathbf{D}_l$  in certain steps. Not only for warm-up, this stage is also used for estimating  $\hat{\rho}$  in (17). In the selection stage, we conduct SGD against  $\mathbf{D}_u$  using  $\mathbf{w}_1$  as the initial solution. At each iteration  $t$ , we sample  $n_t = m\gamma^{t-1}$  training examples from  $\mathbf{D}_u$ , where  $m > 1$  is a parameter defined in (24). We compute the stochastic gradients according to (13):

$$\mathbf{g}_t = \frac{\sum_{i=1}^{n_t} I(f_u(\mathbf{w}_t; \xi_{t,i}^u) \leq \rho_t) \nabla f_u(\mathbf{w}_t; \xi_{t,i}^u)}{\sum_{i=1}^{n_t} I(f_u(\mathbf{w}_t; \xi_{t,i}^u) \leq \rho_t)}. \quad (18)$$

Since  $N_l$  is small, in practice we can also construct the stochastic gradient by using all labeled data as

$$\mathbf{g}_t = \frac{\sum_{i=1}^{n_t - N_l} I(f_u(\mathbf{w}_t; \xi_{t,i}^u) \leq \rho_t) \nabla f_u(\mathbf{w}_t; \xi_{t,i}^u)}{N_l + \sum_{i=1}^{n_t - N_l} I(f_u(\mathbf{w}_t; \xi_{t,i}^u) \leq \rho_t)} + \frac{\sum_{i=1}^{N_l} \nabla f_s(\mathbf{w}_t; \xi_{t,i})}{N_l + \sum_{i=1}^{n_t - N_l} I(f_u(\mathbf{w}_t; \xi_{t,i}^u) \leq \rho_t)}, \quad (19)$$

where  $\xi_{t,i}^u = (x_{t,i}^u, y_{t,i}^u) \in \mathbf{D}_u$  and  $\xi_{t,i} = (x_{t,i}, y_{t,i}) \in \mathbf{D}_l$ . The solution is then updated by mini-batch SGD, whose update step is given by

$$\mathbf{w}_{t+1} = \mathbf{w}_t - \eta \mathbf{g}_t. \quad (20)$$

The detailed updating steps of the proposed algorithm are presented in Algorithm 1, which called SSL with Dynamic Thresholding (Dash).

## 5 Convergence Result

To establish the convergence result of the proposed Dash algorithm, we need to give some preliminaries. Recall that the training examples for the labeled data  $\mathbf{D}_l$  follow the distribution  $\mathcal{P}$ , and we aim to minimize the optimization problem (1). For the examples coming from the unlabeled data  $\mathbf{D}_u$ , suppose it is a mixture of two distributions,  $\mathcal{P}$  and  $\mathcal{Q}$ . More specifically, with a probability  $q$ , we will sample an example from  $\mathcal{P}$  and with a probability  $1 - q$  sample from  $\mathcal{Q}$ :

$$\xi \sim q\mathcal{P} + (1 - q)\mathcal{Q}, \text{ where } \xi \in \mathbf{D}_u, q \in (0, 1). \quad (21)$$

We define the objective function  $B(\mathbf{w})$  as the expected loss for distribution  $\mathcal{Q}$ , i.e.

$$B(\mathbf{w}) := \mathbb{E}_{\xi \sim \mathcal{Q}} [f(\mathbf{w}; \xi)]. \quad (22)$$

For the simplicity of convergence analysis, we do not consider the weak and strong augmentations, i.e., let  $f_s = f_u = f$  in (12) and (13). Without loss of generality, we assume that our loss function is non-negative and is bounded by 1, i.e.  $f(\mathbf{w}; \xi) \in [0, 1]$  for any  $\mathbf{w}$  and  $\xi$ . Then by (1) and (22), we have  $F(\mathbf{w}) \in [0, 1]$  and  $B(\mathbf{w}) \in [0, 1]$ . In order to differentiate the two distribution, we follow the idea of Tsybakov noisy condition [Mammen et al., 1999, Tsybakov, 2004], and assume, for any solution  $\mathbf{w}$ , if  $F(\mathbf{w}) \leq a$ , then

$$\mathbb{E}_{\xi \sim \mathcal{Q}} [I_{\{\xi: f(\mathbf{w}; \xi) \leq F(\mathbf{w})\}}(\xi)] \leq bA^\theta(\mathbf{w}), \quad (23)$$

where  $I_S(\xi)$  is an indicator function,  $\theta \geq 1$ , and  $b$  is constant.

Finally, we made a few more assumptions that are commonly used in the studies of non-convex optimization (e.g., deep learning) [Ghadimi and Lan, 2013, Yuan et al., 2019]. Throughout this paper, we also make the assumptions on the problem (1) as follows.

**Assumption 1.** *Assume the following conditions hold:*

(i) The stochastic gradient  $\nabla f(\mathbf{w}; \xi)$  is unbiased, i.e.,

$$\mathbb{E}_{\xi \sim \mathcal{P}}[\nabla f(\mathbf{w}; \xi)] = \nabla F(\mathbf{w}),$$

and there exists a constant  $G > 0$ , such that

$$\|\nabla f(\mathbf{w}; \xi)\| \leq G.$$

(ii)  $F(\mathbf{w})$  is smooth with a  $L$ -Lipchitz continuous gradient, i.e., it is differentiable and there exists a constant  $L > 0$  such that

$$\|\nabla F(\mathbf{w}) - \nabla F(\mathbf{u})\| \leq L\|\mathbf{w} - \mathbf{u}\|, \forall \mathbf{w}, \mathbf{u} \in \mathbb{R}^d.$$

Assumption 1 (i) assures that the stochastic gradient of the objective function is unbiased and the gradient of  $f(\mathbf{w}; \xi)$  in terms of  $\mathbf{w}$  is upper bounded. Assumption 1 (ii) says the objective function is  $L$ -smooth, and it has an equivalent expression which is  $\forall \mathbf{w}, \mathbf{u} \in \mathbb{R}^d$ ,

$$F(\mathbf{w}) - F(\mathbf{u}) \leq \langle \nabla F(\mathbf{u}), \mathbf{w} - \mathbf{u} \rangle + \frac{L}{2} \|\mathbf{w} - \mathbf{u}\|^2.$$

We now introduce an important property regarding  $F(\mathbf{w})$ , i.e. the Polyak-Łojasiewicz (PL) condition [Polyak, 1963] of  $F(\mathbf{w})$ .

**Assumption 2.** There exists  $\mu > 0$  such that

$$2\mu(F(\mathbf{w}) - F(\mathbf{w}_*)) \leq \|\nabla F(\mathbf{w})\|^2, \forall \mathbf{w} \in \mathbb{R}^d.$$

This PL property has been theoretically and empirically observed in training deep neural networks [Allen-Zhu et al., 2019, Yuan et al., 2019]. This condition is widely used to establish convergence in the literature of non-convex optimization, please see [Yuan et al., 2019, Wang et al., 2019, Karimi et al., 2016, Li and Li, 2018, Charles and Papailiopoulos, 2018] and references therein.

Now, we are ready to provide the theoretical result for Dash. Without loss of generality, let  $F(\mathbf{w}_*) = 0$  in the analysis. Please note that this is a common property observed in training deep neural networks [Zhang et al., 2017, Allen-Zhu et al., 2019, Du et al., 2019, Arora et al., 2019, Chizat et al., 2019, Hastie et al., 2019, Yun et al., 2019]. The following theorem states the convergence guarantee of the proposed Dash algorithm. We include its proof in the Appendix.

**Theorem 1.** Under Assumptions 1 and 2, suppose that  $C > 1$  and  $F(\mathbf{w}_*) = 0$ , for any  $\delta \in (0, 1)$ ,  $\eta_0 L \leq 1$ ,  $\eta L \leq 1$ , let  $T_0 = \frac{\log(2F(\mathbf{w}_0)/a)}{\log(1/(1-\eta_0\mu))}$ ,  $m_0 = \frac{4G^2}{\delta\mu a}$ ,

$$m = \left\lceil \max \left( \sqrt{\frac{\log(2/\delta)}{q^2}}, \sqrt{\frac{\log(2/\delta)}{(1-q)^2}}, \sqrt{\frac{\log(2/\delta)}{q(1-C^{-1})^2}} \right) \right\rceil, \quad (24)$$

$$\hat{\rho} = \max \left\{ a, \frac{4G^2(1+\delta b_0 m)}{\delta\mu a_0 m} \right\} \quad (25)$$

in Algorithm 1, then with a probability  $1 - (4T + 1)\delta$ , we have  $F(\mathbf{w}_{T+1}) \leq \hat{\rho}\gamma^{-T}$ .

**Remark.** We can see from the above result that one can set the iteration number  $T$  to be large enough to ensure the convergence of Dash. Specifically, in order to have an  $\epsilon$  optimization error, one can set  $T = \log(\hat{\rho}/\epsilon)/\log(\gamma)$ , then  $F(\mathbf{w}_{T+1}) \leq \epsilon$ . The total sample complexity of Dash is  $T_0 m_0 + \sum_{t=1}^T m \gamma^{t-1} \leq T_0 m_0 + \frac{m \gamma^T}{\gamma-1} = T_0 m_0 + \frac{m \hat{\rho}}{\epsilon(\gamma-1)} = O(1/\epsilon)$ . This rate matches the result of supervised learning in [Karimi et al., 2016] when analyzing the standard SGD under Assumptions 1 and 2.

Table 1: Comparison of top-1 testing error rates for different methods using Wide ResNet-28-2 for CIFAR-10, Wide ResNet-28-8 for CIFAR-100 (in %, mean  $\pm$  standard deviation).

Algorithm	CIFAR-10			CIFAR-100		
	40 labels	250 labels	4000 labels	400 labels	2500 labels	10000 labels
$\Pi$ -Model	-	54.26 $\pm$ 3.97	14.01 $\pm$ 0.38	-	57.25 $\pm$ 0.48	37.88 $\pm$ 0.11
Pseudo-Labeling	-	49.78 $\pm$ 0.43	16.09 $\pm$ 0.28	-	57.38 $\pm$ 0.46	36.21 $\pm$ 0.19
Mean Teacher	-	32.32 $\pm$ 2.30	9.19 $\pm$ 0.19	-	53.91 $\pm$ 0.57	35.83 $\pm$ 0.24
MixMatch	47.54 $\pm$ 11.50	11.05 $\pm$ 0.86	6.42 $\pm$ 0.10	67.61 $\pm$ 1.32	39.94 $\pm$ 0.37	28.31 $\pm$ 0.33
UDA	29.05 $\pm$ 5.93	8.82 $\pm$ 1.08	4.88 $\pm$ 0.18	59.28 $\pm$ 0.88	33.13 $\pm$ 0.22	24.50 $\pm$ 0.25
ReMixMatch	19.10 $\pm$ 9.64	5.44 $\pm$ 0.05	4.72 $\pm$ 0.13	<b>44.28<math>\pm</math>2.06</b>	27.43 $\pm$ 0.31	23.03 $\pm$ 0.56
RYS (UDA)	-	5.53 $\pm$ 0.17	4.75 $\pm$ 0.28	-	-	-
RYS (FixMatch)	-	5.05 $\pm$ 0.12	4.35 $\pm$ 0.06	-	-	-
FixMatch (CTA)	11.39 $\pm$ 3.35	5.07 $\pm$ 0.33	4.31 $\pm$ 0.15	49.95 $\pm$ 3.01	28.64 $\pm$ 0.24	23.18 $\pm$ 0.11
<b>Dash (CTA, ours)</b>	<b>9.16<math>\pm</math>4.31</b>	4.78 $\pm$ 0.12	4.13 $\pm$ 0.06	44.83 $\pm$ 1.36	27.85 $\pm$ 0.19	22.77 $\pm$ 0.21
FixMatch (RA)	13.81 $\pm$ 3.37	5.07 $\pm$ 0.65	4.26 $\pm$ 0.05	48.85 $\pm$ 1.75	28.29 $\pm$ 0.11	22.60 $\pm$ 0.12
<b>Dash (RA, ours)</b>	13.22 $\pm$ 3.75	<b>4.56<math>\pm</math>0.13</b>	<b>4.08<math>\pm</math>0.06</b>	44.76 $\pm$ 0.96	<b>27.18<math>\pm</math>0.21</b>	<b>21.97<math>\pm</math>0.14</b>

## 6 Experiments

In this section, we present some experimental results for image classification tasks. To evaluate the efficacy of Dash, we compare it with several state-of-the-art (SOTA) baselines on several standard SSL image classification benchmarks including CIFAR-10, CIFAR-100 [Krizhevsky and Hinton, 2009], SVHN [Netzer et al., 2011], and STL-10 [Coates et al., 2011]. Specifically, SOTA baselines are MixMatch [Berthelot et al., 2019b], UDA [Xie et al., 2020a], ReMixMatch [Berthelot et al., 2019a], FixMatch [Sohn et al., 2020] and the algorithm RYS from [Ren et al., 2020]<sup>3</sup>. Besides,  $\Pi$ -Model [Rasmus et al., 2015], Pseudo-Labeling [Lee, 2013] and Mean Teacher [Tarvainen and Valpola, 2017] are included in the comparison.

### 6.1 Data-sets

The original CIFAR data-sets have 50,000 training images and 10,000 testing images of  $32\times 32$  resolutions, and CIFAR-10 has 10 classes containing 6,000 images each, while CIFAR-100 has 100 classes containing 600 images each. The original SVHN data-set has 73,257 digits for training and 26,032 digits for testing, and the total number of classes is 10. The original STL-10 data set has 5,000 labeled images from 10 classes and 100,000 unlabeled images, which contains out-of-distribution unlabeled images.

Following by [Sohn et al., 2020], we train ten benchmarks with different settings: CIFAR-10 with 4, 25, or 400 labels per class, CIFAR-100 with 4, 25, or 100 labels per class, SVHN with 4, 25, or 100 labels per class, and the STL-10 data set. For example, the benchmark CIFAR-10 with 4 labels per class means that there are 40 labeled images in CIFAR-10 and the remaining images are unlabeled, and then we denote this data set by CIFAR-10 with 40 labels. For fair comparison, same sets of labeled images from CIFAR, SVHN and STL-10 were used for the proposed Dash method and other baselines in all experiments.

### 6.2 Models and Hyper-parameters

We use the Wide ResNet-28-2 model [Zagoruyko and Komodakis, 2016] as the backbone for CIFAR-10 and SVHN, Wide ResNet-28-8 for CIFAR-100, and Wide ResNet-37-2 for STL-10. In the proposed Dash, we use

<sup>3</sup>Since the authors did not name their algorithm, we use RYS to denote their algorithm for simplicity, where RYS is the combination of initials for last names of the authors.

Table 2: Comparison of top-1 testing error rates for different methods using Wide ResNet-28-2 for SVHN and Wide ResNet-37-2 for STL-10 (in %, mean  $\pm$  standard deviation).

Algorithm	SVHN			STL-10
	40 labels	250 labels	1000 labels	1000 labels
II-Model	-	18.96 $\pm$ 1.92	7.54 $\pm$ 0.36	26.23 $\pm$ 0.82
Pseudo-Labeling	-	20.21 $\pm$ 1.09	9.94 $\pm$ 0.61	27.99 $\pm$ 0.83
Mean Teacher	-	3.57 $\pm$ 0.11	3.42 $\pm$ 0.07	21.43 $\pm$ 2.39
MixMatch	42.55 $\pm$ 14.53	3.98 $\pm$ 0.23	3.50 $\pm$ 0.28	10.41 $\pm$ 0.61
UDA	52.63 $\pm$ 20.51	5.69 $\pm$ 2.76	2.46 $\pm$ 0.24	7.66 $\pm$ 0.56
ReMixMatch	3.34 $\pm$ 0.20	2.92 $\pm$ 0.48	2.65 $\pm$ 0.08	5.23 $\pm$ 0.45
RYS (UDA)	-	2.45 $\pm$ 0.08	2.32 $\pm$ 0.06	-
RYS (FixMatch)	-	2.63 $\pm$ 0.23	2.34 $\pm$ 0.15	-
FixMatch (CTA)	7.65 $\pm$ 7.65	2.64 $\pm$ 0.64	2.36 $\pm$ 0.19	5.17 $\pm$ 0.63
<b>Dash (CTA, ours)</b>	<b>3.14<math>\pm</math>1.60</b>	<b>2.38<math>\pm</math>0.29</b>	<b>2.14<math>\pm</math>0.09</b>	<b>3.96<math>\pm</math>0.25</b>
FixMatch (RA)	3.96 $\pm$ 2.17	2.48 $\pm$ 0.38	2.28 $\pm$ 0.11	7.98 $\pm$ 1.50
<b>Dash (RA, ours)</b>	<b>3.03<math>\pm</math>1.59</b>	<b>2.17<math>\pm</math>0.10</b>	<b>2.03<math>\pm</math>0.06</b>	<b>7.26<math>\pm</math>0.40</b>

FixMatch<sup>4</sup> as our pipeline to generate pseudo labels and to construct supervised and unsupervised losses. We employ CTAugment (CTA) [Cubuk et al., 2019] and RandAugment (RA) [Cubuk et al., 2020] for the strong augmentation scheme following by [Sohn et al., 2020]. Similar to [Sohn et al., 2020], we use the same training protocol such as optimizer, learning rate schedule, data preprocessing, random seeds, and so on.

The total number of training epochs is set to be 1024 and the mini-batch size is fixed as 64. For the value of weight decay, we use  $5 \times 10^{-4}$  for CIFAR-10, SVHN and STL-10,  $1 \times 10^{-3}$  for CIAR-100. The SGD with momentum parameter of 0.9 is employed as the optimizer. The cosine learning rate decay schedule [Loshchilov and Hutter, 2017] is used as [Sohn et al., 2020]. The initial learning rate is set to be 0.06 for all data-sets. We use (18) to compute stochastic gradients.

At the first 10 epochs, we do not implement the selection scheme and thus the algorithm uses all selected training examples, meaning that the threshold is infinite, i.e.,  $\rho_t = \infty$ . After that, we use the threshold to select unlabeled examples, and we choose  $\gamma = 1.27$  in  $\rho_t$  to reduce the dynamic threshold until its value to be 0.05. That is to say, in practice we give a minimal value of dynamic threshold, which is 0.05<sup>5</sup>. We fix the constant  $C$  as 1.0001 and estimate the value of  $\hat{\rho}$  by using (17). We decay the dynamic threshold every 9 epochs. We use the predicted label distribution as soft label during the training and it is sharpened by adjusting its temperature of 0.5, which is similar to MixMatch. Once the dynamic threshold is reduced to 0.05, we turn it to one-hot label in the training since the largest label probability is close to 1.

### 6.3 Results

We report the top-1 testing error rates of the proposed Dash along within other baselines for CIFAR in Table 1 and for SVHN and STL-10 in Table 2, where all the results of baselines are from [Sohn et al., 2020] except that the results of RYS are from [Ren et al., 2020]. All top-1 testing error rates are averaged over 5 independent random trails with their standard deviations using the same random seeds as baselines used.

We can see from the results that the proposed Dash method has the best performance on CIFAR-10, SVHN and STL-10. For CIFAR-100, the proposed Dash is comparable to ReMixMatch, where ReMixMatch performs a bit better on 400 labels and Dash using RA is a bit better on 2500 labels and 10000 labels. This reason is that the proposed Dash uses FixMatch as its pipeline, and ReMixMatch uses distribution alignment (DA) to encourages the model to predict balanced class distribution (the class distribution of CIFAR-100

<sup>4</sup>In our experiments, the FixMatch codebase is used: <https://github.com/google-research/fixmatch>

<sup>5</sup>In practice, we use  $\rho_t = \max\{\rho_t, 0.05\}$ .

Table 3: Comparison of top-1 testing error rates for different values of  $\gamma$  on CIFAR-10 (in %).

$\gamma$	1.01	1.1	1.2	1.3
250 labels	4.85	<b>4.76</b>	4.99	4.82
4000 labels	4.39	4.28	<b>4.11</b>	4.31

Table 4: Comparison of top-1 testing error rates for PL and Dash with PL on CIFAR-10 (in %).

Algorithm	PL	Dash-PL
250 labels	49.78	<b>46.90</b>
4000 labels	16.09	<b>15.59</b>

is balanced), while FixMatch and Dash do not use DA. We further conduct Dash with DA technique on CIFAR-100 with 400 labels, and the top-1 testing error rate is 43.31%, which is better than ReMixMatch (44.28%). We also find that Dash performs well on the data set with out-of-distribution unlabeled images, i.e., STL-10. The result in Table 2 shows that Dash with CTA has the SOTA performance of 3.96% on top-1 testing error rate.

Besides, the proposed Dash can always outperform FixMatch, showing that the use of dynamic threshold is important to the overall performance. We find the proposed Dash has large improvement when the labeled examples is small (the data-sets with 4 labels per classes), comparing to FixMatch. By using CTA, on CIFAR-100 with 400 labels, on CIFAR-10 with 40 labels, and on SVHN with 40 labels, the proposed Dash method outperforms FixMatch result more than 19%, 10%, and 58% in the terms of top-1 testing error rate, respectively. While by using RA, the corresponding improved rates are 4%, 8%, and 23% respectively. These results reveal that the dynamic unlabeled example selection is an important term in SSL when the labeled data is small.

## 6.4 Ablation study

In this subsection, we provide two ablation studies using data sets CIFAR-10 with 250 labels and CIFAR-10 with 4000 labels. The first one is to use different  $\gamma$  in the dynamic threshold, and the second one is to change FixMatch to Pseudo-Labeling as the pseudo label generator in Dash.

**Different values of  $\gamma$ .** Since  $\gamma$  is a key component of the dynamic threshold, we conduct an ablation study on different values of  $\gamma$  in Dash. For simplicity, we only implement the CTA case. We try four different values of  $\gamma \in \{1.01, 1.1, 1.2, 1.3\}$  and summarize the results in Table 3. Comparing these results with that in Table 1, we will find that the choice of  $\gamma = 1.27$  in the previous subsection is not the best one. The results also show that Dash is not so sensitive to  $\gamma$  in a certain range.

**Dash with Pseudo-Labeling.** Since Dash can be integrated with many existing SSL methods, we use Pseudo-Labeling (PL) [Lee, 2013] as the pipeline to generate pseudo labels in Dash. The results are listed in Table 4, showing that Dash can improve PL, especially when the labeled images is small.

## 7 Conclusion

We propose a method Dash that dynamically selects unlabeled data examples to train learning models. Its selection strategy keeps the unlabeled data whose loss value does not exceed a dynamic threshold at each optimization step. The proposed Dash method is a generic scheme that can be easily integrated with existing SSL methods. We demonstrate the use of dynamically selecting unlabeled data can help to the performance of existing SSL method FixMatch in the semi-supervised image classification benchmarks, indicating the importance of dynamic threshold in SSL. The theoretical analysis shows the convergence guarantee of the proposed Dash under the non-convex optimization setting.

## Acknowledgements

The authors would like to thank the anonymous ICML 2021 reviewers for their helpful comments.

## References

- Zeyuan Allen-Zhu, Yuanzhi Li, and Zhao Song. A convergence theory for deep learning via overparameterization. In *International Conference on Machine Learning*, pages 242–252, 2019.
- Sanjeev Arora, Simon Du, Wei Hu, Zhiyuan Li, and Ruosong Wang. Fine-grained analysis of optimization and generalization for overparameterized two-layer neural networks. In *International Conference on Machine Learning*, pages 322–332, 2019.
- Philip Bachman, Ouais Alsharif, and Doina Precup. Learning with pseudo-ensembles. In *Advances in Neural Information Processing Systems*, pages 3365–3373, 2014.
- Henry S Baird. Document image defect models. In *Structured Document Image Analysis*, pages 546–556. Springer, 1992.
- Maria-Florina Balcan and Avrim Blum. A pac-style model for learning from labeled and unlabeled data. In *International Conference on Computational Learning Theory*, pages 111–126. Springer, 2005.
- Akshay Balsubramani and Yoav Freund. Optimally combining classifiers using unlabeled data. In *Conference on Learning Theory*, pages 211–225, 2015.
- Shai Ben-David, Tyler Lu, and Dávid Pál. Does unlabeled data provably help? worst-case analysis of the sample complexity of semi-supervised learning. In *Conference on Learning Theory*, pages 33–44, 2008.
- David Berthelot, Nicholas Carlini, Ekin D Cubuk, Alex Kurakin, Kihyuk Sohn, Han Zhang, and Colin Raffel. Remixmatch: Semi-supervised learning with distribution matching and augmentation anchoring. In *International Conference on Learning Representations*, 2019a.
- David Berthelot, Nicholas Carlini, Ian Goodfellow, Nicolas Papernot, Avital Oliver, and Colin A Raffel. Mixmatch: A holistic approach to semi-supervised learning. In *Advances in Neural Information Processing Systems*, pages 5050–5060, 2019b.
- Avrim Blum and Tom Mitchell. Combining labeled and unlabeled data with co-training. In *Proceedings of Annual Conference on Computational Learning Theory*, pages 92–100, 1998.
- Olivier Chapelle, Bernhard Scholkopf, and Alexander Zien. *Semi-Supervised Learning (1st edition)*. Cambridge: The MIT Press, 2006.
- Zachary Charles and Dimitris Papailiopoulos. Stability and generalization of learning algorithms that converge to global optima. In *International Conference on Machine Learning*, pages 745–754, 2018.
- Minmin Chen, Kilian Q Weinberger, and Yixin Chen. Automatic feature decomposition for single view co-training. In *International Conference on Machine Learning*, pages 953–960, 2011.
- Lenaic Chizat, Edouard Oyallon, and Francis Bach. On lazy training in differentiable programming. In *Advances in Neural Information Processing Systems*, pages 2937–2947, 2019.
- Fan Chung and Linyuan Lu. Concentration inequalities and martingale inequalities: a survey. *Internet Mathematics*, 3(1):79–127, 2006.
- Adam Coates, Andrew Ng, and Honglak Lee. An analysis of single-layer networks in unsupervised feature learning. In *International Conference on Artificial Intelligence and Statistics*, pages 215–223, 2011.

- Fabio G Cozman, Ira Cohen, and Marcelo C Cirelo. Semi-supervised learning of mixture models. In *International Conference on Machine Learning*, pages 99–106, 2003.
- Ekin D Cubuk, Barret Zoph, Dandelion Mane, Vijay Vasudevan, and Quoc V Le. Autoaugment: Learning augmentation strategies from data. In *Proceedings of the IEEE Conference on Computer Vision and Pattern Recognition*, pages 113–123, 2019.
- Ekin D Cubuk, Barret Zoph, Jonathon Shlens, and Quoc V Le. Randaugment: Practical automated data augmentation with a reduced search space. In *Proceedings of the IEEE Conference on Computer Vision and Pattern Recognition Workshops*, pages 702–703, 2020.
- Simon Du, Jason Lee, Haochuan Li, Liwei Wang, and Xiyu Zhai. Gradient descent finds global minima of deep neural networks. In *International Conference on Machine Learning*, pages 1675–1685, 2019.
- Peter Flach. *Machine learning: the art and science of algorithms that make sense of data*. Cambridge University Press, 2012.
- Saeed Ghadimi and Guanghui Lan. Stochastic first-and zeroth-order methods for nonconvex stochastic programming. *SIAM Journal on Optimization*, 23(4):2341–2368, 2013.
- Saeed Ghadimi, Guanghui Lan, and Hongchao Zhang. Mini-batch stochastic approximation methods for nonconvex stochastic composite optimization. *Mathematical Programming*, 155(1-2):267–305, 2016.
- Ian Goodfellow, Yoshua Bengio, and Aaron Courville. *Deep learning*. MIT press, 2016.
- Yves Grandvalet and Yoshua Bengio. Semi-supervised learning by entropy minimization. In *Advances in Neural Information Processing Systems*, pages 529–536, 2005.
- Lan-Zhe Guo, Zhen-Yu Zhang, Yuan Jiang, Yu-Feng Li, and Zhi-Hua Zhou. Safe deep semi-supervised learning for unseen-class unlabeled data. In *International Conference on Machine Learning*, pages 3897–3906, 2020.
- Mohamed Farouk Abdel Hady and Friedhelm Schwenker. Semi-supervised learning. In *Handbook on Neural Information Processing*, pages 215–239. Springer, 2013.
- Trevor Hastie, Andrea Montanari, Saharon Rosset, and Ryan J Tibshirani. Surprises in high-dimensional ridgeless least squares interpolation. *arXiv preprint arXiv:1903.08560*, 2019.
- Ryuichiro Hataya and Hideki Nakayama. Unifying semi-supervised and robust learning by mixup. 2019.
- Hamed Karimi, Julie Nutini, and Mark Schmidt. Linear convergence of gradient and proximal-gradient methods under the polyak-lojasiewicz condition. In *Joint European Conference on Machine Learning and Knowledge Discovery in Databases*, pages 795–811. Springer, 2016.
- Jesse H Krijthe and Marco Loog. Projected estimators for robust semi-supervised classification. *Machine Learning*, 106(7):993–1008, 2017.
- Alex Krizhevsky and Geoffrey Hinton. Learning multiple layers of features from tiny images. *Master’s thesis, Technical report, University of Tronto*, 2009.
- Samuli Laine and Timo Aila. Temporal ensembling for semi-supervised learning. In *International Conference on Learning Representations*, 2017.
- Dong-Hyun Lee. Pseudo-label: The simple and efficient semi-supervised learning method for deep neural networks. In *In ICML Workshop on Challenges in Representation Learning*, 2013.
- Junnan Li, Richard Socher, and Steven CH Hoi. Dividemix: Learning with noisy labels as semi-supervised learning. *International Conference on Learning Representations*, 2020.

- Yu-Feng Li and Zhi-Hua Zhou. Improving semi-supervised support vector machines through unlabeled instances selection. In *Proceedings of the AAAI Conference on Artificial Intelligence*, pages 386–391, 2011a.
- Yu-Feng Li and Zhi-Hua Zhou. Towards making unlabeled data never hurt. In *International Conference on Machine Learning*, pages 1081–1088, 2011b.
- Yu-Feng Li and Zhi-Hua Zhou. Towards making unlabeled data never hurt. *IEEE Transactions on Pattern Analysis and Machine Intelligence*, 37(1):175–188, 2015.
- Yu-Feng Li, Han-Wen Zha, and Zhi-Hua Zhou. Learning safe prediction for semi-supervised regression. In *Proceedings of the Thirty-First AAAI Conference on Artificial Intelligence*, pages 2217–2223, 2017.
- Yu-Feng Li, Lan-Zhe Guo, and Zhi-Hua Zhou. Towards safe weakly supervised learning. *IEEE Transactions on Pattern Analysis and Machine Intelligence*, 43(1):334–346, 2021.
- Zhize Li and Jian Li. A simple proximal stochastic gradient method for nonsmooth nonconvex optimization. In *Advances in Neural Information Processing Systems*, pages 5564–5574, 2018.
- Marco Loog. Contrastive pessimistic likelihood estimation for semi-supervised classification. *IEEE Transactions on Pattern Analysis and Machine Intelligence*, 38(3):462–475, 2015.
- Ilya Loshchilov and Frank Hutter. Sgdr: Stochastic gradient descent with warm restarts. *International Conference on Learning Representations*, 2017.
- Enno Mammen, Alexandre B Tsybakov, et al. Smooth discrimination analysis. *The Annals of Statistics*, 27(6):1808–1829, 1999.
- Geoffrey J McLachlan. Iterative reclassification procedure for constructing an asymptotically optimal rule of allocation in discriminant analysis. *Journal of the American Statistical Association*, 70(350):365–369, 1975.
- Alexander Mey and Marco Loog. Improvability through semi-supervised learning: a survey of theoretical results. *arXiv preprint arXiv:1908.09574*, 2019.
- Ishan Misra, Abhinav Shrivastava, and Martial Hebert. Watch and learn: Semi-supervised learning for object detectors from video. In *Proceedings of the IEEE Conference on Computer Vision and Pattern Recognition*, pages 3593–3602, 2015.
- Takeru Miyato, Shin-ichi Maeda, Masanori Koyama, and Shin Ishii. Virtual adversarial training: a regularization method for supervised and semi-supervised learning. *IEEE Transactions on Pattern Analysis and Machine Intelligence*, 41(8):1979–1993, 2018.
- Yuval Netzer, Tao Wang, Adam Coates, Alessandro Bissacco, Bo Wu, and Andrew Y. Ng. Reading digits in natural images with unsupervised feature learning. 2011.
- Avital Oliver, Augustus Odena, Colin A Raffel, Ekin Dogus Cubuk, and Ian Goodfellow. Realistic evaluation of deep semi-supervised learning algorithms. In *Advances in Neural Information Processing Systems*, pages 3235–3246, 2018.
- Boris Teodorovich Polyak. Gradient methods for minimizing functionals. *Zhurnal Vychislitel’noi Matematiki i Matematicheskoi Fiziki*, 3(4):643–653, 1963.
- Antti Rasmus, Harri Valpola, Mikko Honkala, Mathias Berglund, and Tapani Raiko. Semi-supervised learning with ladder networks. In *Neural Information Processing Systems*, pages 3546–3554, 2015.
- Zhongzheng Ren, Raymond Yeh, and Alexander Schwing. Not all unlabeled data are equal: learning to weight data in semi-supervised learning. *Advances in Neural Information Processing Systems*, 33, 2020.

- Chuck Rosenberg, Martial Hebert, and Henry Schneiderman. Semi-supervised self-training of object detection models. In *Proceedings of the 7th IEEE Workshops on Application of Computer Vision*, pages 29–36, 2005.
- Mehdi Sajjadi, Mehran Javanmardi, and Tolga Tasdizen. Regularization with stochastic transformations and perturbations for deep semi-supervised learning. In *Advances in Neural Information Processing Systems*, pages 1163–1171, 2016.
- Jürgen Schmidhuber. Deep learning in neural networks: An overview. *Neural networks*, 61:85–117, 2015.
- Vikas Sindhwani and David S Rosenberg. An rkhs for multi-view learning and manifold co-regularization. In *International Conference on Machine Learning*, pages 976–983, 2008.
- Aarti Singh, Robert Nowak, and Jerry Zhu. Unlabeled data: Now it helps, now it doesn’t. In *Advances in Neural Information Processing Systems*, pages 1513–1520, 2009.
- Kihyuk Sohn, David Berthelot, Chun-Liang Li, Zizhao Zhang, Nicholas Carlini, Ekin D Cubuk, Alex Kurakin, Han Zhang, and Colin Raffel. Fixmatch: Simplifying semi-supervised learning with consistency and confidence. In *Advances in Neural Information Processing Systems*, pages 596–608, 2020.
- Antti Tarvainen and Harri Valpola. Mean teachers are better role models: Weight-averaged consistency targets improve semi-supervised deep learning results. In *Advances in Neural Information Processing Systems*, pages 1195–1204, 2017.
- Alexander B Tsybakov. Optimal aggregation of classifiers in statistical learning. *The Annals of Statistics*, 32(1):135–166, 2004.
- Joseph Turian, Lev Ratinov, and Yoshua Bengio. Word representations: a simple and general method for semi-supervised learning. In *Proceedings of Annual Meeting of the Association for Computational Linguistics*, pages 384–394, 2010.
- Jesper E Van Engelen and Holger H Hoos. A survey on semi-supervised learning. *Machine Learning*, 109(2):373–440, 2020.
- Jiao Wang, Si-wei Luo, and Xian-hua Zeng. A random subspace method for co-training. In *Proceedings of IEEE International Joint Conference on Neural Networks*, pages 195–200, 2008.
- Wei Wang and Zhi-Hua Zhou. A new analysis of co-training. In *International Conference on Machine Learning*, pages 1135–1142, 2010.
- Zhe Wang, Kaiyi Ji, Yi Zhou, Yingbin Liang, and Vahid Tarokh. Spiderboost and momentum: Faster variance reduction algorithms. In *Advances in Neural Information Processing Systems*, pages 2403–2413, 2019.
- Qizhe Xie, Zihang Dai, Eduard Hovy, Thang Luong, and Quoc Le. Unsupervised data augmentation for consistency training. In *Advances in Neural Information Processing Systems*, pages 6256–6268, 2020a.
- Qizhe Xie, Minh-Thang Luong, Eduard Hovy, and Quoc V Le. Self-training with noisy student improves imagenet classification. In *Proceedings of the IEEE Conference on Computer Vision and Pattern Recognition*, pages 10687–10698, 2020b.
- David Yarowsky. Unsupervised word sense disambiguation rivaling supervised methods. In *Proceedings of Annual Meeting of the Association for Computational Linguistics*, pages 189–196, 1995.
- Dong Yu, Balakrishnan Varadarajan, Li Deng, and Alex Acero. Active learning and semi-supervised learning for speech recognition: A unified framework using the global entropy reduction maximization criterion. *Computer Speech & Language*, 24(3):433–444, 2010.

- Shipeng Yu, Balaji Krishnapuram, Harald Steck, R Bharat Rao, and Rómer Rosales. Bayesian co-training. In *Advances in Neural Information Processing Systems*, pages 1665–1672, 2008.
- Zhuoning Yuan, Yan Yan, Rong Jin, and Tianbao Yang. Stagewise training accelerates convergence of testing error over SGD. In *Advances in Neural Information Processing Systems*, pages 2604–2614, 2019.
- Chulhee Yun, Suvrit Sra, and Ali Jadbabaie. Small ReLU networks are powerful memorizers: a tight analysis of memorization capacity. In *Advances in Neural Information Processing Systems*, pages 15558–15569, 2019.
- Sergey Zagoruyko and Nikos Komodakis. Wide residual networks. *British Machine Vision Conference*, 2016.
- Chiyuan Zhang, Samy Bengio, Moritz Hardt, Benjamin Recht, and Oriol Vinyals. Understanding deep learning requires rethinking generalization. *International Conference on Learning Representations*, 2017.
- Zhi-Hua Zhou and Ming Li. Tri-training: Exploiting unlabeled data using three classifiers. *IEEE Transactions on Knowledge and Data Engineering*, 17(11):1529–1541, 2005.
- Xiaojin Zhu and Andrew B Goldberg. Introduction to semi-supervised learning. *Synthesis Lectures on Artificial Intelligence and Machine Learning*, 3(1):1–130, 2009.
- Xiaojin Jerry Zhu. Semi-supervised learning literature survey. Technical report, Technical Report, University of Wisconsin-Madison Department of Computer Sciences, 2005.

## A Proof of Theorem 1

In this section, we present the proof of our main theoretical result. To this end, we divide the analysis into two parts, with the first part devoted to examining the properties of  $\mathbf{w}_1$  learned in the first step and the second part devoted to the convergence for the iterations. As the setting of SSL, we assume that the number of unlabeled data is large, i.e.,  $N_u$  is sufficiently large.

### A.1 Properties of Solution $\mathbf{w}_1$

We first give the property of  $\mathbf{w}_1$  in the following lemma, whose proof can be found in the Appendix.

**Lemma 1.** *Given  $\delta \in (0, 1)$ , run the Warm-up Stage of Algorithm 1 with  $\eta_0 \leq \frac{1}{L}$ ,  $T_0 = \frac{\log(2F(\mathbf{w}_0)/a)}{\log(1/(1-\eta_0\mu))}$  and  $m_0 = \frac{4G^2}{\delta\mu a}$ , then with a probability  $1 - 5\delta$  we have  $F(\mathbf{w}_1) \leq \hat{\rho}$ .*

*Proof.* Since the objective function  $F(\mathbf{u})$  has a Lipschitz continuous gradient in Assumption 1 (ii), we have

$$\begin{aligned}
 & F(\mathbf{u}_{t+1}) - F(\mathbf{u}_t) \\
 & \leq \langle \nabla F(\mathbf{u}_t), \mathbf{u}_{t+1} - \mathbf{u}_t \rangle + \frac{L}{2} \|\mathbf{u}_{t+1} - \mathbf{u}_t\|^2 \\
 & \stackrel{(a)}{=} \frac{\eta_0}{2} \|\nabla F(\mathbf{u}_t) - \tilde{\mathbf{g}}_t\|^2 - \frac{\eta_0}{2} (\|\nabla F(\mathbf{u}_t)\|^2 + (1 - \eta_0 L) \|\tilde{\mathbf{g}}_t\|^2) \\
 & \stackrel{(b)}{\leq} \frac{\eta_0}{2} \|\nabla F(\mathbf{u}_t) - \tilde{\mathbf{g}}_t\|^2 - \eta_0 \mu F(\mathbf{u}_t),
 \end{aligned} \tag{26}$$

where (a) follows the update of  $\mathbf{u}_{t+1} = \mathbf{u}_t - \eta_0 \tilde{\mathbf{g}}_t$ ; (b) follows from Assumption 2 and  $\eta_0 L \leq 1$ . Since  $\mathbb{E}[\tilde{\mathbf{g}}_t] = \nabla F(\mathbf{u}_t)$  and

$$\begin{aligned}
 & \mathbb{E} [\|\tilde{\mathbf{g}}_t - \nabla F(\mathbf{u}_t)\|^2] \\
 & = \frac{1}{m_0^2} \sum_{i=1}^{m_0} \mathbb{E} [\|\nabla f(\mathbf{u}_t; \xi_i^t) - \nabla F(\mathbf{u}_t)\|^2] \\
 & \leq \frac{4G^2}{m_0}, \quad (\text{Assumption 1 (i)})
 \end{aligned} \tag{27}$$

using concentration inequality in Lemma 4 of [Ghadimi et al., 2016], we have with a probability  $1 - 5\delta$ ,

$$\|\tilde{\mathbf{g}}_t - \nabla F(\mathbf{u}_t)\|^2 \leq \frac{4G^2}{\delta m_0}. \tag{28}$$

Using the above bound  $\|\tilde{\mathbf{g}}_t - \nabla F(\mathbf{u}_t)\|$ , we can further bound  $F(\mathbf{u}_T)$  by using (26) and (27) as

$$\begin{aligned}
 F(\mathbf{u}_{T_0}) & \leq (1 - \eta_0 \mu) F(\mathbf{u}_{T_0-1}) + \frac{2\eta_0 G^2}{\delta m_0} \\
 & \leq (1 - \eta_0 \mu)^{T_0} F(\mathbf{u}_0) + \frac{2\eta_0 G^2}{\delta m_0} \sum_{i=0}^{T_0-1} (1 - \eta_0 \mu)^i \\
 & \leq (1 - \eta_0 \mu)^{T_0} F(\mathbf{u}_0) + \frac{2G^2}{\delta m_0 \mu},
 \end{aligned}$$

which implies

$$F(\mathbf{w}_1) \leq (1 - \eta_0 \mu)^{T_0} F(\mathbf{w}_0) + \frac{2G^2}{\delta m_0 \mu}. \tag{29}$$

By selecting  $T_0 \geq \frac{\log(2F(\mathbf{w}_0)/a)}{\log(1/(1-\eta_0\mu))}$  and  $m_0 \geq \frac{4G^2}{\delta\mu a}$ , we have

$$F(\mathbf{w}_1) \leq a. \quad (30)$$

Therefore the condition in (23) is applicable in this case. On the other hand, by the definition of  $\hat{\rho}$  in (25), we know, with a probability  $1 - 5\delta$ , that

$$F(\mathbf{w}_1) \leq \hat{\rho}. \quad (31)$$

□

## A.2 Analysis of Iterative Algorithm

The key to our analysis is to show that for each iteration  $t$ , with a high probability, we have  $F(\mathbf{w}_t) \leq \hat{\rho}\gamma^{-(t-1)}$ . We will prove this statement by induction. Before we carry out our analysis, we define a few important constants

$$\beta = \max \left( \sqrt{\frac{\log(2/\delta)}{2q^2m}}, \sqrt{\frac{\log(2/\delta)}{2(1-q)^2m}} \right), \quad (32)$$

$$\alpha = \sqrt{\frac{\log(2/\delta)}{qm(1-C^{-1})^2}} \geq \sqrt{\frac{\log(2/\delta)}{2qm(1-\beta)(1-C^{-1})^2}}, \quad (33)$$

$$a_0 = (1-C^{-1})(1-\beta)(1-\alpha)q, \quad (34)$$

$$b_0 = 2((1-q)(1+\beta)b\hat{\rho}^\theta + \log(1/\delta)), \quad (35)$$

$$b_1 = \frac{b_0}{a_0}. \quad (36)$$

When  $t = 1$ , we have  $F(\mathbf{w}_1) \leq \hat{\rho}$  according to Lemma 1. At each iteration  $t$ , given the solution  $\mathbf{w}_t$ , according to our inductive assumption, with a probability  $1 - (4t + 1)\delta$ , we have

$$F(\mathbf{w}_t) \leq \hat{\rho}\gamma^{-(t-1)}, \quad (37)$$

For the  $n_t = m\gamma^{t-1}$  training examples sampled from  $\mathbf{D}_u$ , we divide it into two sets for the analysis use only, i.e. set  $\mathcal{A}_t$  that includes examples sampled from  $\mathcal{P}$  and set  $\mathcal{B}_t$  that includes examples sampled from  $\mathcal{Q}$ . We furthermore denote by  $\mathcal{A}_t^\rho$  and  $\mathcal{B}_t^\rho$  the subset of examples in  $\mathcal{A}_t$  and  $\mathcal{B}_t$  whose loss is smaller than the given threshold  $\rho_t$ , i.e.

$$\mathcal{A}_t^\rho = \{\xi \in \mathcal{A}_t : f(\mathbf{w}_t; \xi) \leq \rho_t\}, \quad (38)$$

$$\mathcal{B}_t^\rho = \{\xi \in \mathcal{B}_t : f(\mathbf{w}_t; \xi) \leq \rho_t\}, \quad (39)$$

where  $\rho_t = C\hat{\rho}\gamma^{-(t-1)}$  with  $C > 1$ . Evidently, the samples used for computing  $g_t$  is the union of  $\mathcal{A}_t^\rho$  and  $\mathcal{B}_t^\rho$ . The following result bounds the size of  $\mathcal{A}_t^\rho$  and  $\mathcal{B}_t^\rho$ . With a probability  $1 - 4\delta$ , we have

$$|\mathcal{A}_t^\rho| \geq a_0m\gamma^{(t-1)}, \quad |\mathcal{B}_t^\rho| \leq b_0m, \quad (40)$$

where  $a_0$  and  $b_0$  are defined in (34) and (35). Using the Hoeffding's inequality, we have, with a probability  $1 - 2\delta$ ,

$$|\mathcal{A}_t| \geq qn_t \left( 1 - \sqrt{\frac{\log(2/\delta)}{2q^2n_t}} \right) \stackrel{(32)}{\geq} qn_t(1-\beta), \quad (41)$$

$$|\mathcal{B}_t| \leq (1-q)n_t \left( 1 + \sqrt{\frac{\log(2/\delta)}{2(1-q)^2n_t}} \right) \stackrel{(32)}{\leq} (1-q)n_t(1+\beta). \quad (42)$$

Furthermore, using Markov inequality, we have

$$\begin{aligned}
\Pr_{\xi \sim \mathcal{P}}(f(\mathbf{w}_t; \xi) \leq \rho_t) &= 1 - \Pr_{\xi \sim \mathcal{P}}(f(\mathbf{w}_t; \xi) \geq \rho_t) \\
&\stackrel{\text{Markov inequality}}{\geq} 1 - \frac{\mathbb{E}_{\xi \sim \mathcal{P}}[f(\mathbf{w}_t; \xi)]}{\rho_t} \\
&= 1 - \frac{F(\mathbf{w}_t)}{C\hat{\rho}\gamma^{-(t-1)}} \\
&\stackrel{(a)}{\geq} 1 - \frac{\hat{\rho}\gamma^{-(t-1)}}{C\hat{\rho}\gamma^{-(t-1)}} = 1 - C^{-1}, \tag{43}
\end{aligned}$$

where (a) uses the fact that  $F(\mathbf{w}_t) \leq \hat{\rho}\gamma^{-(t-1)}$ . Using the property in (43), we can bound the size of  $\mathcal{A}_t^\rho$  by Hoeffding's inequality, i.e., with a probability  $1 - 2\delta$ , we have

$$|\mathcal{A}_t^\rho| \geq (1 - C^{-1}) |\mathcal{A}_t| \left( 1 - \sqrt{\frac{\log(2/\delta)}{2(1 - C^{-1})^2 |\mathcal{A}_t|}} \right) \stackrel{(32)(33)}{\geq} (1 - C^{-1})(1 - \beta)(1 - \alpha)qn_t := a_0 m \gamma^{t-1}, \tag{44}$$

where  $a_0$  is defined in (34). Using the inequality in (23) we know

$$\begin{aligned}
\Pr_{\xi \sim \mathcal{Q}}(f(\mathbf{w}_t; \xi) \leq \rho_t) &= \Pr_{\xi \sim \mathcal{Q}}(f(\mathbf{w}_t; \xi) \leq C\hat{\rho}\gamma^{-(t-1)}) \\
&\stackrel{(a)}{\leq} \Pr_{\xi \sim \mathcal{Q}}(f(\mathbf{w}_t; \xi) \leq \hat{\rho}\gamma^{-(t-1)}) \\
&\stackrel{(b)}{\leq} \Pr_{\xi \sim \mathcal{Q}}(f(\mathbf{w}_t; \xi) \leq F(\mathbf{w}_t)) \\
&= \mathbb{E}_{\xi \sim \mathcal{Q}}[I(f(\mathbf{w}_t; \xi) \leq F(\mathbf{w}_t))] \\
&\stackrel{(23)}{\leq} bA^\theta F(\mathbf{w}_t) \stackrel{(c)}{\leq} b(\hat{\rho}\gamma^{-(t-1)})^\theta, \tag{45}
\end{aligned}$$

where (a) is due to  $C > 1$ ; (b) and (c) are due to  $F(\mathbf{w}_t) \leq \hat{\rho}\gamma^{-(t-1)}$ . Using the property in (45), we can bound the expectation of  $|\mathcal{B}_t^\rho|$  given  $|\mathcal{B}_t|$ , i.e.,

$$\begin{aligned}
\mathbb{E}_{\xi \sim \mathcal{Q}}[|\mathcal{B}_t^\rho|] &= \mathbb{E}_{\xi_i \sim \mathcal{Q}} \left[ \sum_{i=1}^{|\mathcal{B}_t|} I(f(\mathbf{w}_t; \xi_i) \leq \rho_t) \right] \\
&= \sum_{i=1}^{|\mathcal{B}_t|} \mathbb{E}_{\xi_i \sim \mathcal{Q}} [I(f(\mathbf{w}_t; \xi_i) \leq \rho_t)] \\
&= \sum_{i=1}^{|\mathcal{B}_t|} \Pr_{\xi_i \sim \mathcal{Q}}(f(\mathbf{w}_t; \xi_i) \leq \rho_t) \\
&\stackrel{(45)}{\leq} |\mathcal{B}_t| b(\hat{\rho}\gamma^{-(t-1)})^\theta. \tag{46}
\end{aligned}$$

We can bound the size of  $\mathcal{B}_t^\rho$  by a concentration inequality in Theorem 8 of [Chung and Lu, 2006], with a probability  $1 - 2\delta$ ,

$$\begin{aligned}
|\mathcal{B}_t^\rho| &\leq \mathbb{E}_{\xi \sim \mathcal{Q}}[|\mathcal{B}_t^\rho|] + \frac{1}{3} \log(1/\delta) + \sqrt{\frac{1}{9} \log^2(1/\delta) + 2 \log(1/\delta) \mathbb{E}_{\xi \sim \mathcal{Q}}[|\mathcal{B}_t^\rho|]} \\
&\stackrel{(46)}{\leq} |\mathcal{B}_t| b(\hat{\rho}\gamma^{-(t-1)})^\theta + \frac{1}{3} \log(1/\delta) + \sqrt{\frac{1}{9} \log^2(1/\delta) + 2 \log(1/\delta) |\mathcal{B}_t| b(\hat{\rho}\gamma^{-(t-1)})^\theta} \\
&\leq 2|\mathcal{B}_t| b(\hat{\rho}\gamma^{-(t-1)})^\theta + 2 \log(1/\delta) \\
&\stackrel{(42)}{\leq} 2(1 - q)m\gamma^{t-1}(1 + \beta)b(\hat{\rho}\gamma^{-(t-1)})^\theta + 2 \log(1/\delta) \\
&\leq 2((1 - q)(1 + \beta)b\hat{\rho}^\theta + \log(1/\delta)) m := b_0 m, \tag{47}
\end{aligned}$$

where  $b_0$  is defined in (35). Therefore, we complete the proof of (40).

As indicated in (44) and (47),  $|\mathcal{A}_t^\rho|$  increases exponentially over iteration while  $|\mathcal{B}_t^\rho|$  remains upper bounded by a constant. It implies that our dynamically adjusted threshold help us select more and more examples from the unlabeled data that are relevant to the labeled data. In the same time, the number of mistakes we made in the selection process remain to be at most a constant. As a result, our optimization is able to make significant progress by using the selected examples from the unlabeled data. Below we will show that with a high probability,  $F(\mathbf{w}_{t+1}) \leq \widehat{\rho}\gamma^{-t}$ , the key step of the inductive analysis. Finally, we will prove that with a probability  $1 - (4t + 1)\delta$ , we have

$$F(\mathbf{w}_{t+1}) \leq \widehat{\rho}\gamma^{-t}.$$

To this end, using the notation of  $\mathcal{A}_t^\rho$  and  $\mathcal{B}_t^\rho$ , we can rewrite  $\mathbf{g}_t$  as

$$\mathbf{g}_t = (1 - b_t)\mathbf{g}_t^a + b_t\mathbf{g}_t^b,$$

where  $\mathbf{g}_t^a = \frac{1}{|\mathcal{A}_t^\rho|} \sum_{\xi \in \mathcal{A}_t^\rho} \nabla f(\mathbf{w}_t; \xi)$ ,  $\mathbf{g}_t^b = \frac{1}{|\mathcal{B}_t^\rho|} \sum_{\xi \in \mathcal{B}_t^\rho} \nabla f(\mathbf{w}_t; \xi)$ , and  $b_t$  is the proportion of samples from  $\mathcal{B}_t^\rho$  that

$$b_t = \frac{|\mathcal{B}_t^\rho|}{|\mathcal{A}_t^\rho| + |\mathcal{B}_t^\rho|} \leq \frac{|\mathcal{B}_t^\rho|}{|\mathcal{A}_t^\rho|} \leq \frac{b_0}{a_0} \gamma^{-(t-1)} = b_1 \gamma^{-(t-1)}. \quad (48)$$

Following the classical analysis of non-convex optimization, since  $F(\mathbf{w})$  is  $L$ -smooth by Assumption 1 (ii), we have

$$\begin{aligned} & F(\mathbf{w}_{t+1}) - F(\mathbf{w}_t) \\ & \leq \langle \nabla F(\mathbf{w}_t), \mathbf{w}_{t+1} - \mathbf{w}_t \rangle + \frac{L}{2} \|\mathbf{w}_{t+1} - \mathbf{w}_t\|^2 \\ & \stackrel{(a)}{=} \frac{\eta}{2} \|\nabla F(\mathbf{w}_t) - \mathbf{g}_t\|^2 - \frac{\eta}{2} (\|\nabla F(\mathbf{w}_t)\|^2 + (1 - \eta L) \|\mathbf{g}_t\|^2) \\ & \stackrel{(b)}{\leq} \frac{\eta}{2} ((1 - b_t) \|\nabla F(\mathbf{w}_t) - \mathbf{g}_t^a\|^2 + b_t \|\nabla F(\mathbf{w}_t) - \mathbf{g}_t^b\|^2) - \frac{\eta}{2} (\|\nabla F(\mathbf{w}_t)\|^2 + (1 - \eta L) \|\mathbf{g}_t\|^2) \\ & \stackrel{(c)}{\leq} \frac{\eta}{2} ((1 - b_t) \|\nabla F(\mathbf{w}_t) - \mathbf{g}_t^a\|^2 + 4b_t G^2) - \eta \mu F(\mathbf{w}_t), \end{aligned}$$

where (a) follows the update of  $\mathbf{w}_{t+1} = \mathbf{w}_t - \eta \mathbf{g}_t$ ; (b) is due to the definition of  $\mathbf{g}_t$  and the convexity of  $\|\cdot\|^2$ ; (c) follows from Assumption 2, Assumption 1 (i), and  $\eta L \leq 1$ . Since  $\mathbb{E}_{\xi \sim \mathcal{P}}[\nabla f(\mathbf{w}; \xi)] = \nabla F(\mathbf{w})$  and

$$\begin{aligned} & \mathbb{E}_{\xi \sim \mathcal{P}} \left[ \|\mathbf{g}_t^a - \nabla F(\mathbf{w}_t)\|^2 \right] \\ & = \mathbb{E}_{\xi \sim \mathcal{P}} \left[ \left\| \frac{1}{|\mathcal{A}_t^\rho|} \sum_{\xi \in \mathcal{A}_t^\rho} \nabla f(\mathbf{w}_t; \xi) - \nabla F(\mathbf{w}_t) \right\|^2 \right] \\ & = \frac{1}{|\mathcal{A}_t^\rho|^2} \sum_{\xi \in \mathcal{A}_t^\rho} \mathbb{E}_{\xi \sim \mathcal{P}} \left[ \|\nabla f(\mathbf{w}_t; \xi) - \nabla F(\mathbf{w}_t)\|^2 \right] \\ & \leq \frac{4G^2}{|\mathcal{A}_t^\rho|}, \quad (\text{Assumption 1 (i)}) \end{aligned}$$

using concentration inequality in Lemma 4 of [Ghadimi et al., 2016], we have with a probability  $1 - 5\delta$ ,

$$\|\mathbf{g}_t^a - \nabla F(\mathbf{w}_t)\|^2 \leq \frac{4G^2}{\delta |\mathcal{A}_t^\rho|} \stackrel{(40)}{\leq} \frac{4G^2}{\delta a_0 m \gamma^{t-1}}.$$

Using the above bound  $\|\mathbf{g}_t^a - \nabla F(\mathbf{w})\|$ , we can further bound  $F(\mathbf{w}_{t+1}) - F(\mathbf{w}_t)$  as

$$\begin{aligned}
& F(\mathbf{w}_{t+1}) - F(\mathbf{w}_t) \\
& \leq \frac{\eta}{2} \left( (1 - b_t) \frac{4G^2}{\delta a_0 m \gamma^{t-1}} + 4b_t G^2 \right) - \eta \mu F(\mathbf{w}_t) \\
& \stackrel{(48)}{\leq} \frac{\eta}{2} \left( \frac{4G^2}{\delta a_0 m \gamma^{t-1}} + 4G^2 b_1 \gamma^{-(t-1)} \right) - \eta \mu F(\mathbf{w}_t) \\
& = 2\eta G^2 \left( \frac{1}{\delta a_0 m} + b_1 \right) \gamma^{-(t-1)} - \eta \mu F(\mathbf{w}_t)
\end{aligned} \tag{49}$$

where  $b_1$  is defined in (36). Hence, we have

$$F(\mathbf{w}_{t+1}) \leq (1 - \eta \mu) F(\mathbf{w}_t) + 2\eta G^2 \left( \frac{1}{\delta a_0 m} + b_1 \right) \gamma^{-(t-1)} \tag{50}$$

Let select  $\gamma = \frac{1}{1 - \eta \mu / 2}$ , we know by using (37) the inequality (50) will become

$$\begin{aligned}
F(\mathbf{w}_{t+1}) & \leq \gamma (1 - \eta \mu) \hat{\rho} \gamma^{-t} + 2\eta \gamma G^2 \left( \frac{1}{\delta a_0 m} + b_1 \right) \gamma^{-t} \\
& = \left( 1 - \frac{\eta \mu / 2}{1 - \eta \mu / 2} \right) \hat{\rho} \gamma^{-t} \\
& \quad + \frac{\eta \mu / 2}{1 - \eta \mu / 2} \frac{4G^2}{\mu} \left( \frac{1}{\delta a_0 m} + b_1 \right) \gamma^{-t}
\end{aligned}$$

By the setting of  $\hat{\rho}$  we have

$$F(\mathbf{w}_{t+1}) \leq \hat{\rho} \gamma^{-t}. \tag{51}$$

Therefore, we complete the proof by induction.